

Structure and hydrogen bonding in CaSiD_{1+x} : Issues about covalent bondingH. Wu,^{1,2,*} W. Zhou,^{1,3} T. J. Udovic,¹ J. J. Rush,^{1,2} and T. Yildirim^{1,3}¹NIST Center for Neutron Research, National Institute of Standards and Technology, 100 Bureau Drive, MS 8562, Gaithersburg, Maryland 20899-8562, USA²Department of Materials Science and Engineering, University of Maryland, College Park, Maryland 20742-2115, USA³Department of Materials Science and Engineering, University of Pennsylvania, 3231 Walnut Street, Philadelphia, Pennsylvania 19104-6272, USA

(Received 11 July 2006; revised manuscript received 4 September 2006; published 7 December 2006)

We report here our high-resolution neutron powder diffraction and neutron vibrational spectroscopy study of CaSiD_{1+x} along with first-principles calculations, which reveal the deuterium structural arrangements and bonding in this novel alloy hydride. Both the structural and spectroscopic results show that, for $x > 0$, D atoms start occupying a Ca_2Si interstitial site. The corresponding Si-D bond length is determined to be 1.82 Å, fully 0.24 Å larger than predicted by theory. Thus, our neutron measurements are at odds with the strongly covalent Si-H bonding in CaSiH_{1+x} that such calculations suggest, a result which may have implications for a number of ongoing studies of metal-hydrogen systems destabilized by Si alloying.

DOI: 10.1103/PhysRevB.74.224101

PACS number(s): 61.12.-q, 63.20.-e, 71.15.Mb, 81.05.Je

I. INTRODUCTION

Recently there has been hydrogen-storage interest in the intermetallic compound, CaSi, which has been found to reversibly absorb more than one hydrogen per CaSi formula unit.¹ While both x-ray diffraction and first-principles calculations have shed light on the general structure of CaSiH_{1+x} (Refs. 1 and 2), no neutron powder diffraction (NPD) or neutron vibrational spectroscopy (NVS) studies have thus far been reported to elucidate the exact interstitial locations and bonding of the H atoms within the rearranged CaSi lattice, and in so doing, rigorously test recent theoretical predictions.² High-resolution NPD combined with NVS provide a powerful probe of the structure, dynamics, and bonding states in metal-hydride materials. Hence, in the present work, we report our neutron scattering results compared with first-principles phonon calculations for CaSiD_{1+x} . The neutron results, particularly our structural study, are not consistent with the strongly covalent Si-H bonding in this system predicted by theory.

II. EXPERIMENTAL SECTION

A $\text{CaSiD}_{1.2}$ powder sample was synthesized by (i) first forming CaSi via evacuation of a ball-milled (400 rpm for 30 min) CaH_2 (Aldrich,³ 99.9%) + Si (Alfa Aesar 99.999%) 1:1 stoichiometric mixture at 873 K for 5 h, and (ii) deutering this CaSi by reaction with gas-phase D_2 (99.999%) at 9 MPa and 473 K. CaSiD was obtained by controlled evacuative desorption of D_2 from $\text{CaSiD}_{1.2}$ at 353–373 K. CaSi, CaSiD , and $\text{CaSiD}_{1.2}$ crystal structures were determined using high-resolution NPD. In addition, D optical phonon spectra of CaSiD and $\text{CaSiD}_{1.2}$ were measured by NVS. All sample handling was performed in a He-filled glovebox to avoid oxidation reactions.

All measurements were undertaken at the NIST Center for Neutron Research. The NPD measurements were performed with the BT-1 high-resolution powder diffractometer⁴ using

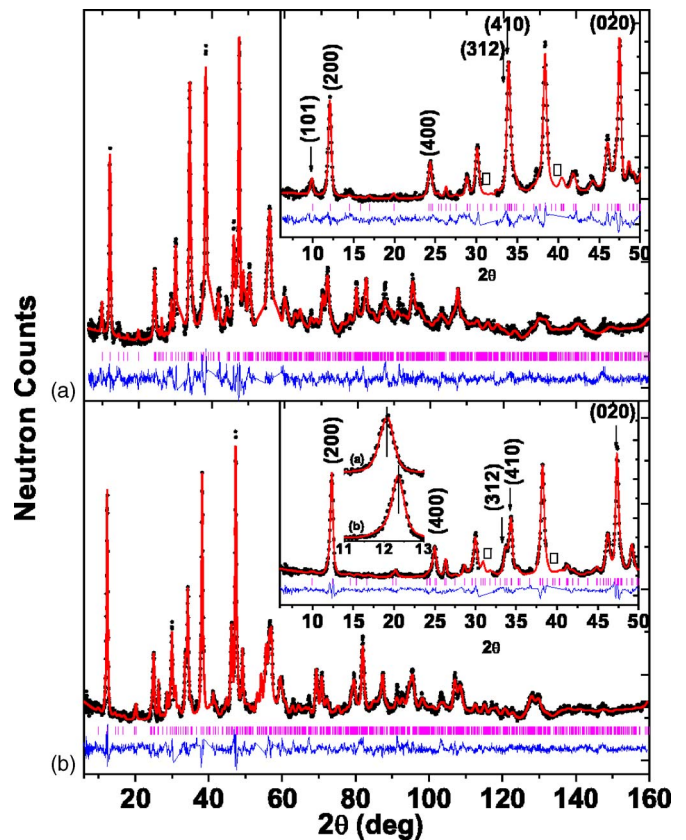


FIG. 1. (Color online) Experimental (dots), calculated (line), and difference NPD profiles for (a) $\text{CaSiD}_{1.2}$ and (b) CaSiD . The low-angle portions of the diffraction patterns are also presented in insets. An additional small inset shows expanded-scale (200) peaks for (a) $\text{CaSiD}_{1.2}$ and (b) CaSiD more clearly indicating the peak shift. Squares indicated the positions of some impurity peaks that are not related to the $\text{CaSiD}_{1.2}$ and CaSiD phases. These impurity peaks were removed from the NPD patterns for clarity.

the Cu(311) monochromator at a wavelength of 1.5403(2) Å. Rietveld structural refinements were done using the GSAS package.⁵ The NVS measurements were performed with the BT-4 filter-analyzer neutron spectrometer⁶ using the Cu(220) monochromator.

III. RESULTS AND DISCUSSION

The effectiveness of the ball-milling method for producing single-phase CaSi was demonstrated by the good agreement between the published CaSi (CrB-type) structure⁷ and the refinement model fits of the NPD data collected on the resultant alloy. Structure refinements on CaSiD_{1.2} were performed within the space group *Pnma* (No. 62) with the initial atomic positions as suggested from the recent calculations of Ohba *et al.*² The experimental, fitted, and difference profiles of the NPD patterns for the final refined structures of CaSiD_{1.2} are shown in Fig. 1. The refined atomic positions yield excellent fits for the observed profiles of all the peaks. The final refined crystallographic parameters are summarized in Tables I and II. The results are generally consistent with the recent x-ray diffraction study.² No significant structural changes or phase transformations were evident from the dif-

TABLE I. Crystallographic data for CaSiD_y at 298 K.

Space group	$y=1.19 \approx 1.2$	$y=0.97 \approx 1$
	<i>Pnma</i>	<i>Pnma</i>
a (Å)	14.56846(14)	14.20912(32)
b (Å)	3.82028(23)	3.83380(25)
c (Å)	11.20921(12)	11.46781(27)
V (Å ³)	623.856(2)	624.709(6)
R_p	0.0438	0.0415
R_{wp}	0.0519	0.0511
R_F^2	0.0416	0.0442
χ^2	1.666	1.869

fraction patterns at 10 K and 298 K. Structure refinement using the NPD data for CaSiD (Fig. 1) also revealed a *Pnma* unit cell (Tables I and II), which differs from the CrB-type structure of CaSiH (space group *Cmcm*) suggested by Ohba *et al.*² From Fig. 1, visible changes in peak intensities [e.g., (101)], shapes [e.g., (312) and (410)], and positions [e.g., (200) and (020)] clearly show structure variations with D concentration (also see the lattice parameter changes in Table

TABLE II. Refined structural parameters for CaSiD_y at 298 K.

CaSiD _{1.2} (<i>N.B.</i> : refined stoichiometry yields CaSiD _{1.19})											
Atom	Site	Occupancy	x	y	z	U_{11}	U_{22}	U_{33}	U_{12}	U_{13}	U_{23}
Ca1	4c	1.00	0.3646(2)	0.25	-0.0257(3)	1.311(5)	1.414(2)	1.241(5)	0	-0.074(4)	0
Ca2	4c	1.00	0.3312(1)	0.25	0.3594(2)	1.311(5)	1.414(2)	1.241(5)	0	-0.074(4)	0
Ca3	4c	1.00	0.1892(1)	0.75	0.1492(3)	1.311(5)	1.414(2)	1.241(5)	0	-0.074(4)	0
Si1	4c	1.00	0.0355(3)	0.25	0.0369(2)	2.395(1)	0.286(3)	1.129(4)	0	1.433(3)	0
Si2	4c	1.00	0.5786(2)	0.25	0.2103(1)	2.395(1)	0.286(3)	1.129(4)	0	1.433(3)	0
Si3	4c	1.00	0.4600(2)	0.75	0.1999(1)	2.395(1)	0.286(3)	1.129(4)	0	1.433(3)	0
D1	4c	0.992(1)	0.2642(2)	0.25	0.1702(1)	1.809(1)	0.462(6)	1.832(1)	0	-1.329(4)	0
D2	4c	0.984(2)	0.2661(4)	0.75	-0.0143(2)	1.809(1)	0.462(6)	1.832(1)	0	-1.329(4)	0
D3	4c	1.00 ^a	0.2466(4)	0.75	0.3358(1)	1.809(1)	0.462(6)	1.832(1)	0	-1.329(4)	0
D4	4c	0.590(1)	0.0230(4)	0.25	0.5392(5)	1.809(1)	0.462(6)	1.832(1)	0	-1.329(4)	0
CaSiD (<i>N.B.</i> : refined stoichiometry yields CaSiD _{0.97})											
Atom	Site	Occupancy	x	y	z	U_{11}	U_{22}	U_{33}	U_{12}	U_{13}	U_{23}
Ca1	4c	1.00	0.3629(2)	0.25	-0.0029(3)	2.582(3)	0.546(3)	3.579(2)	0	-3.257(1)	0
Ca2	4c	1.00	0.3466(2)	0.25	0.3467(1)	2.582(3)	0.546(3)	3.579(2)	0	-3.257(1)	0
Ca3	4c	1.00	0.1935(4)	0.75	0.1607(1)	2.582(3)	0.546(3)	3.579(2)	0	-3.257(1)	0
Si1	4c	1.00	0.0451(2)	0.25	0.0182(1)	1.985(4)	1.696(4)	1.872(2)	0	0.307(3)	0
Si2	4c	1.00	0.5344(1)	0.25	0.2523(1)	1.985(4)	1.696(4)	1.872(2)	0	0.307(3)	0
Si3	4c	1.00	0.4717(1)	0.75	0.1891(2)	1.985(4)	1.696(4)	1.872(2)	0	0.307(3)	0
D1	4c	0.977(2)	0.2682(4)	0.25	0.1695(1)	2.815(2)	0.404(1)	2.699(2)	0	-0.938(1)	0
D2	4c	0.989(4)	0.2676(2)	0.75	-0.0037(1)	2.815(2)	0.404(1)	2.699(2)	0	-0.938(1)	0
D3	4c	0.945(2)	0.2364(3)	0.75	0.3395(1)	2.815(2)	0.404(1)	2.699(2)	0	-0.938(1)	0
D4	4c	0 ^b									

^aThe D3 occupancy tended to be slightly larger than 1 during the refinement, and was thus fixed at 1.

^bThe D4 occupancy tended to be slightly negative during the refinement, and was thus fixed at 0. U_{ij} are all $\times 100$ Å². All thermal factors are assumed to be anisotropic and identical for all atoms of the same element.

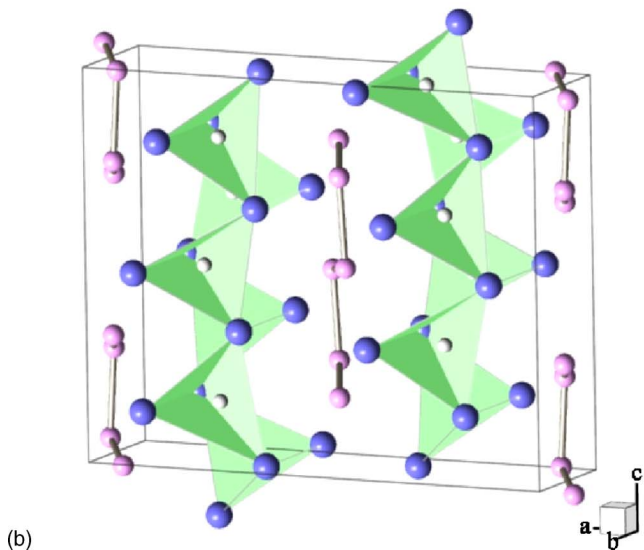
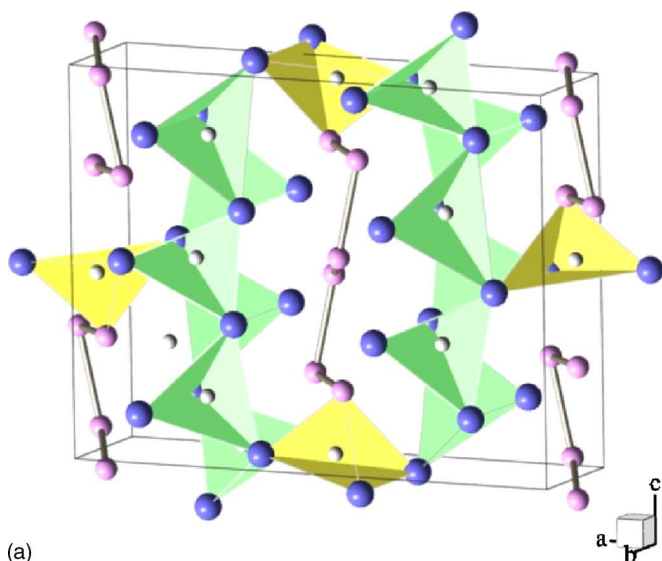


FIG. 2. (Color online) Crystal structure of (a) $\text{CaSiD}_{1.2}$ and (b) CaSiD . The large black spheres, medium gray spheres, and small white spheres represent Ca, Si, and D atoms, respectively. Ca_4 -site tetrahedra are in dark gray; Ca_3Si -site tetrahedra in light gray.

I). The structural models indicate that the intensity of the (101) peak increases with increasing D occupancy of the Ca_3Si (D4) site. The refined deuterium occupancies yield stoichiometries of “ $\text{CaSiD}_{1.19}$ ” and “ $\text{CaSiD}_{0.97}$,” respectively, for the $\text{CaSiD}_{1.2}$ and CaSiD samples, consistent with the measured gravimetric uptakes for the deuterides.

The refined structures of $\text{CaSiD}_{1.2}$ and CaSiD are shown in Fig. 2. For simplicity, anisotropic thermal factors were assumed to be identical for all atoms of the same element. Allowing for the independent refinement of thermal factors for each atom in the unit cell led to similar structural results with only insignificant changes in some of the atomic fractions and no strong correlations between occupancies and thermal factors. Compared to CaSi , the unit cell of $\text{CaSiD}_{1.2}$ expands three times along the c axis (the a axis of CaSi), and the resultant structure has two kinds of D sites with different

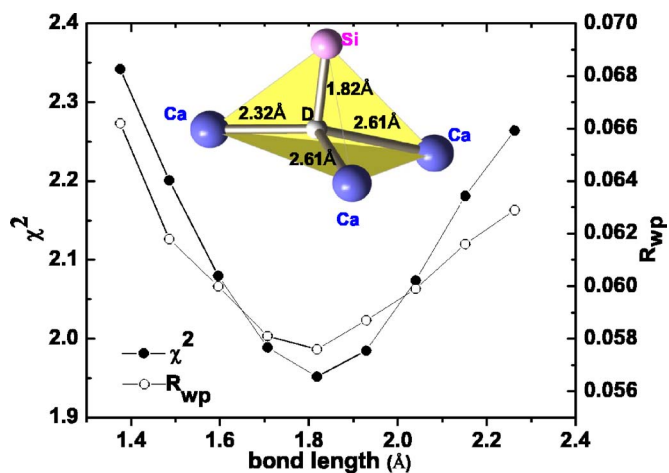


FIG. 3. (Color online) The Rietveld goodness-of-fit parameters χ^2 and R_{wp} vs the $\text{Si}_3\text{-D}_4$ bond length fixed at various values along the $\text{Si}_3\text{-D}_4$ axis as determined by the refined optimal position of D in the Ca_3Si interstices (shown schematically).

nearest neighbors. One kind of D site (the D1, D2, and D3 sites), is defined by four Ca nearest neighbors (Ca_4 sites, 1 per Ca_3Si). These Ca_4 tetrahedra align in a zigzag fashion along the c direction. The Ca-D distances for these sites vary from 2.01 Å to 2.64 Å, in the same range as the Ca-D distances in CaD_2 .⁸ Interestingly, the D1, D2, and D3 sites do not have identical coordination environments. Rather, they reside in slightly different off-centered positions in the Ca_4 interstices.

The second kind of D site (D4) is located close to the center of a triangle of three Ca (Ca_1) atoms as well as one Si (Si_3) atom (Ca_3Si site, 0.33 per Ca_3Si). Since $\text{CaSiD}_{1.2}$ is a D-deficient $\text{CaSiD}_{1.33}$ phase, the D4 sites are found to be partially occupied (59%), presumably in a disordered fashion. The minimum D4-D4 distance is 2.21 Å and the minimum separation between the Ca_4 and Ca_3Si sites is 3.13 Å. A recent theoretical study of $\text{CaSiH}_{1.3}$ by Ohba *et al.*² has concluded that the H atom in the Ca_3Si -type site is covalently bonded to the Si atom with a Si-H bond length of 1.58 Å, close to the 1.48 Å bond length in SiH_4 . Yet, our results indicate that the $\text{Si}_3\text{-D}_4$ distance is 1.82 Å (at 298 K), considerably larger (by ≈ 0.24 Å) than that predicted by Ohba *et al.*, and also consistent with the bond length calculated from the atomic positions tabulated by the same authors from synchrotron x-ray data. Figure 3 shows that fixing this Si-D distance at values either increasingly larger or smaller than 1.82 Å leads to increasing χ^2 and R_{wp} values (i.e., poorer model fits). Similar results are found for calculated deviations in other crystallographic directions. Besides being much larger than the Si-H bond length in SiH_4 , 1.82 Å is also larger than that of any Si-H bond reported for various Si-H cluster, defect, and hydrogenated silicon (1.50–1.56 Å).^{9–11} These experimental results clearly call into question the prediction of Si-H covalency by first-principles calculations.²

The refined structure of CaSiD [Fig. 2(b)] reveals an empty D4 site and essentially full occupancies of the other three Ca_4 -type D sites in the lattice. Compared to $\text{CaSiD}_{1.2}$,

CaSiD retains the $Pnma$ symmetry with a slight shrinkage along the \mathbf{a} axis and slight expansions along the \mathbf{b} and \mathbf{c} axes. Similar to CaSiD_{1,2}, the D1, D2, and D3 sites are located in slightly different off-centered positions in nonidentical, distorted Ca₄ interstices.

To further probe the nature of the deuterium bonding in CaSiD_{1+x}, we have studied the deuterium vibrations in both phases. Figure 4 shows the vibrational spectra for CaSiD_{1+x} measured at 3.5 K. The vibrational peak evident near 63.4 meV for CaSiD_{1,2} is largely absent for CaSiD, matching the disappearance of the (101) diffraction peaks in the corresponding CaSiD pattern. Therefore, this peak can be directly associated with the D4 atoms in the Ca₃Si sites. In addition, the CaSiD_{1,2} spectrum does not reveal any distinct one-phonon peaks associated with stretching modes of the predicted Si-D covalent bond,² which would be expected below 180 meV based on the 180–190 meV stretching energies for Si-D bond lengths near 1.48 Å.^{12–14} This result, however, is obscured somewhat by the broad multiphonon band present in our spectrum combined with the realization that only one-sixth of the total D atoms reside in Ca₃Si sites, meaning that only less than 6% of the integrated phonon intensity is expected to be due to the Si-D stretching modes.

It should be noted that analogous NVS measurements for CaSiH_{1+x} (not shown here) produced similar vibrational spectra with H vibrational energies roughly a factor of $\sqrt{2}$ larger than the corresponding D vibration energies for CaSiD_{1+x}. It is clear that the H and D vibrational spectra exhibit similar complex bands comprised of multiple overlapping peaks, which indicates that they possess the same structures and experience similar structural variations with changing H(D) concentration.

The NV spectrum of CaSiD is well-reproduced (Fig. 4) using first-principles phonon calculations (similar to the formalism of Ohba *et al.*²) within the plane-wave implementation of the generalized gradient approximation to density functional theory (DFT) in the PWSCF package.¹⁵ We used a Vanderbilt-type ultrasoft potential with Perdew-Burke-Ernzerhof exchange correlation. A cutoff energy of 408 eV and a $3 \times 5 \times 3$ k -point mesh were found to be enough for the total energy to converge within 0.5 meV/atom. We first optimized the CaSiD structure. The relaxed atomic positions of CaSiD agreed closely with our experimental values. The phonon calculations were then performed with the optimized structure using the supercell method with finite difference.¹⁶ A supercell of $1a \times 2b \times 1c$ was used and the full dynamical matrix was obtained from a total of 54 symmetry-independent atomic displacements (0.01 Å). The CaSiD NV spectra were computed for a $10 \times 10 \times 10$ q -point grid within the incoherent approximation with instrumental resolution taken into account.^{16,17} More detailed calculations will be presented in a subsequent paper.¹⁸

Since CaSiD_{1,2} possesses partial occupancy of the D4 site, NVS calculations were carried out on structure models with full D4 occupancy, i.e., CaSiD_{1,33} (same symmetry as CaSiD_{1,2} but with 1 D atom/Ca₃Si site) as well as half D4 occupancy, i.e., CaSiD_{1,17} (0.5 D atoms/Ca₃Si site with \mathbf{b} -axis-directed D4 chains comprised of alternating D atoms and vacancies) using the same procedures and methods. Although the latter configuration decreases the overall symme-

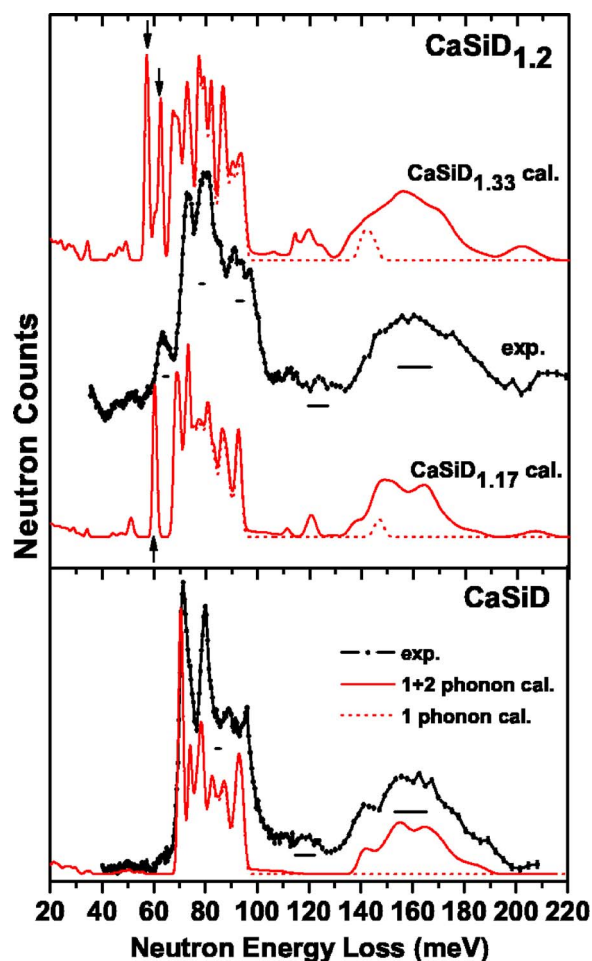


FIG. 4. (Color online) Neutron vibrational spectra of CaSiD_{1,2} and CaSiD. Full width half maximum instrumental resolutions are depicted by the horizontal bars beneath the spectra. Calculated spectra for CaSiD, CaSiD_{1,17}, and CaSiD_{1,33} delineating both 1 phonon (dotted line) and 1+2 phonon (solid line) contributions are shown with the experimental data. The calculated splitting of D4 modes in CaSiD_{1,33} and the single mode for CaSiD_{1,17} (as discussed in the text) are indicated by arrows.

try due to the ordering (No. 26, $Pmc21$), it is useful as a basis for calculating the effect of vacancies on the local bonding within CaSiD_{1+x} structures where $x < 0.33$. Starting with the structure model determined from our NPD data, we obtained optimized structures for both stoichiometries very close to the one containing the 1.58 Å Si-H covalent bonds reported by Ohba *et al.*² It is clear in Fig. 4 that the calculated CaSiD_{1+x} vibrational spectra are noticeably dependent on both the occupation and degree of ordering associated with the Ca₃Si (D4) sites. For example, the calculated CaSiD_{1,33} spectrum indicates that full occupation of the D4 sites causes a splitting of the D4-associated vibrational modes parallel to the plane of the Ca₃ triads at 57.3 and 62.6 meV (indicated by arrows in the figure), presumably due to interactions between nearest-neighbor D4 atoms. This splitting disappears (see Fig. 4), yielding a peak near 60.2 meV for the calculated, vacancy-ordered CaSiD_{1,17} spectrum, which possesses no such nearest-neighbor pairs. The orthogonal Si-D stretching modes (corresponding to the 1.58 Å bond length) are

predicted near 142 meV for $\text{CaSiD}_{1.33}$ and 147 meV for $\text{CaSiD}_{1.17}$.

Compared to calculation, the observed $\text{CaSiD}_{1.2}$ spectrum appears to possess a disordered arrangement of occupied D4 sites as reflected by the significantly broadened D4-related vibrational mode centered near 63.4 meV. Aware that the calculated $\text{CaSiD}_{1.33}$ and $\text{CaSiD}_{1.17}$ NV spectra are not expected to be exactly comparable to that of disordered $\text{CaSiD}_{1.2}$, there are, nonetheless, notable discrepancies in the 50–70 meV region (e.g., lower predicted peak energies) associated with the Ca_3Si -occupied D atoms as well as in the 70–100 meV region mainly associated with the Ca_4 -occupied D atoms. Of particular note is the higher-than-predicted 63.4 meV feature for $\text{CaSiD}_{1.2}$, which is consistent with a D4 atom that is closer to the Ca_3 triad, and therefore, farther from the Si3 atom than calculated by DFT. However, as mentioned earlier, the position of the orthogonal Si-D stretching modes for $\text{CaSiD}_{1.2}$ cannot be definitively determined by the present NVS results due to the multiphonon band.

IV. CONCLUSIONS

In conclusion, for the CaSiD structure, neutron scattering results and DFT calculations are in good agreement both in

terms of structure and dynamics (i.e., the phonon spectrum). However, this is not the case when additional D atoms are added to the structure in the vicinity of the Si atom. The strong disagreement concerning the location and bonding of D atoms in the Ca_3Si interstices raises important questions about the “covalent nature” of the Si-H bonding first suggested in Ref. 2 and also predicted by our own DFT calculations. It is clear that further studies, both experimental and theoretical, are needed to fully understand the nature of the Si-H bonding in this interesting CaSi -hydride phase. A fundamental understanding of the Si-H bonding in the various silicide-based hydrides is critical for the successful theory-driven development of improved hydrogen-storage materials containing Si.

ACKNOWLEDGMENTS

This work was partially supported by DOE through EERE Grant No. DE-AI-01-05EE11104 and BES Grant No. DE-FG02-98ER45701.

*Corresponding author. Electronic address: huiwu@nist.gov

¹M. Aoki, N. Ohba, T. Noritake, and S. Towata, *Appl. Phys. Lett.* **85**, 387 (2004).

²N. Ohba, M. Aoki, T. Noritake, K. Miwa, and S. I. Towata, *Phys. Rev. B* **72**, 075104 (2005).

³Certain commercial suppliers are identified in this paper to foster understanding. Such identification does not imply recommendation or endorsement by the National Institute of Standards and Technology, nor does it imply that the materials or equipment identified are necessarily the best available for the purpose.

⁴J. K. Stalick, E. Prince, A. Santoro, I. G. Schroder, and J. J. Rush, in *Neutron Scattering in Materials Science II*, MRS Symposia Proceedings No. 376, edited by D. A. Neumann, T. P. Russell, and B. J. Wuensch (Materials Research Society, Pittsburgh, PA, 1995), p. 101.

⁵A. C. Larson and R. B. Von Dreele, Report LAUR 86-748, Los Alamos National Laboratory, NM, 1994.

⁶T. J. Udovic, D. A. Neumann, J. Leão, and C. M. Brown, *Nucl. Instrum. Methods Phys. Res. A* **517**, 189 (2004).

⁷W. Rieger and E. Parthe, *Acta Crystallogr.* **22**, 919 (1967).

⁸H. Wu, W. Zhou, T. J. Udovic, J. J. Rush, and T. Yildirim, *J. Alloys Compds.* (to be published).

⁹R. O. Jones, B. W. Clare, and P. J. Jennings, *Phys. Rev. B* **64**, 125203 (2001).

¹⁰B. Tuttle, C. G. Van de Walle, and J. B. Adams, *Phys. Rev. B* **59**, 5493 (1999).

¹¹C. K. Ong and G. K. Khoo, *J. Phys. C* **20**, 419 (1987).

¹²T. K. Gounev, G. A. Guirgis, P. Zhen, and J. R. Durig, *Spectrochim. Acta, Part A* **A56**, 2563 (2000).

¹³E. C. Freeman and W. Paul, *Phys. Rev. B* **18**, 4288 (1978).

¹⁴G. Lucovsky, R. J. Nemanich, and J. C. Knights, *Phys. Rev. B* **19**, 2064 (1979).

¹⁵S. Baroni, A. Dal Corso, S. de Gironcoli, and P. Giannozzi, <http://www.pwscf.org>.

¹⁶T. Yildirim, *Chem. Phys.* **261**, 205 (2000).

¹⁷G. L. Squires, *Introduction to the Theory of Thermal Neutron Scattering* (Dover, New York, 1996).

¹⁸H. Wu, W. Zhou, T. J. Udovic, J. J. Rush, and T. Yildirim (private communication).